Mine Water and the Environment (2022) 41:906–920
https://doi.org/10.1007/s10230-022-00894-3

TECHNICAL ARTICLE

A Hydro-Economic Model for Optimizing Management of Mine Water: A Case Study in the Suancigou Coal Mine, Northwestern China

Wenping Mu[1] · Xiong Wu[2] · Hanghang Ding[3] · Fuqiang Geng[4] · Shuai Yu[3] · Xiao Zhang[2]

Received: 27 April 2020 / Accepted: 25 July 2022 / Published online: 6 September 2022

Abstract

Comprehensive analysis of hydrogeological conditions at a typical coal mine in northwestern China allowed us to establish a groundwater numerical model, which we calibrated using the hydraulic head from observation wells. Then, based on groundwater numerical simulation and operational research theories, we established a hydro-economic mine water management model that was coupled with the numerical model by the response matrix method. The management model took mine dewatering, water supply, and environmental protection into consideration, and realized the maximization economic benefits under the mine's hydraulic constraints. We obtained the unit impulse response function of the management model from the groundwater numerical model according to the superposition principle. Finally, the maximum economic value and optimization of water supply for users were calculated using the management model. Results showed that the management model can reduce the risk of water inrush while also raising lucrative economic income. It can ensure the sustainable supply of water resources, protect the environment, and balance the requirements of mine dewatering, water supply, and environmental protection. Due to the water shortages, fragile environment, and abundance of coal resources in northwestern China, this management model may be widely applicable in this area.

Keywords Mine dewatering · Water supply · Environmental protection · Unit impulse response function · Groundwater numerical simulation

Introduction

China is the biggest producer of coal in the word; annual coal production is about 3.6 billion t, which accounts for ≈ 70% of primary energy production in China (Gu et al. 2016; He et al. 2018; Wu 2014). Because of complex hydrogeological conditions, a large amount of groundwater flows into underground mines; the inflow rate of mine water exceeds 1000 m^3/h in some mines (Feng et al. 2014; Wu 2014; Wu et al. 2005). Mine dewatering totals 7.2 billion t per year in China (Wu 2014; Yin et al. 2016). On average, the mining of 1 kg of coal results in the discharge of about 2 kg of groundwater (Wu 2014).

The utilization ratio of mine water in China is only 20–30% (He et al. 2008; Sun et al. 2012; Wu 2014), which is relatively low. Only a small amount of mine water supports mining operations, such as coal preparation and dust suppression (He et al. 2008). A large amount of contaminated mine water is discharged into nearby rivers, polluting the surface water, groundwater, and soil (Feng et al. 2014; He et al. 2008; Wu et al. 2005; Yin et al. 2016). Some associated environmental problems also appear due to disturbance of the groundwater system by the mine dewatering process: examples include karst collapse, spring disappearance, and vegetation degradation (Lamoreaux et al. 2014; Wu et al. 2000; Yin et al. 2016). In addition, dewatering can affect the water needs of the mine and its surrounding enterprises and residents (Wu et al. 2005, 2006, 2017; Yin et al. 2016).

✉ Xiong Wu
wuxiong@cugb.edu.cn

1 School of Engineering and Technology, China University of Geosciences (Beijing), Beijing 100083, China

2 School of Water Resources and Environment, China University of Geosciences (Beijing), Beijing 100083, China

3 National Engineering Research Center of Coal Mine Water Hazard Controlling, China University of Mining and Technology (Beijing), Beijing 100083, China

4 Key Laboratory of Groundwater Resources and Environment, Shandong Provincial Bureau of Geology and Mineral Resources, Jinan 250014, China

Resolving the contradictory problems of the relationships between mine dewatering, water supply, and environmental protection is therefore extremely difficult (Lamoreaux et al. 2014; Sun et al. 2012; Wu 2014; Wu et al. 2005, 2006, 2017). Management of mine water—including dewatering, water supply and environmental protection—is important for the sustainable development of the coal industry (Hancock and Wolkersdorfer 2012; He et al. 2018; Sun et al. 2012; Wu et al. 2005, 2006). This is especially true in northwestern China, which is characterized by ample coal resources, deficient water resources, and a fragile ecological environment (Feng et al. 2014; He et al. 2018; Wu et al. 2017).

In northwestern China, the typical source of mine water is a fractured aquifer overlying the coal seams (Sun et al. 2012; Wu et al. 2015). In general, the fractured aquifer can be regarded as the equivalent of porous media at a large scale, allowing groundwater movement in it to be approximated by Darcy's law (Panagopoulos 2012; Wu et al. 2009; Wu and Zhou 2008; Zeng et al. 2018). Groundwater numerical models, based on the seepage theory of equivalent porous media, are widely used to simulate water flow in fractures and predict inflow during mining activities (Ardejani et al. 2003; Krcmar and Sracek 2014; Rapantova et al. 2007; Wu et al. 2015; Wu and Zhou 2008; Zeng et al. 2018).

There are two types of groundwater management models commonly used to optimally allocate water resources, environmental geologic problems, and economic gains associated with groundwater exploitation in the development of groundwater resources): hydraulic management and hydraulic–economic management models (Gong et al. 2000; Ma et al. 2004; Singh et al. 2013; Theodossiou 2004; Yin et al. 2016; Zhu 2013; Zhu et al. 2014). The latter takes economic factors into account. A few researchers have proposed using the same two kinds of management models for mine water (Wu et al. 2005, 2006, 2010; Yin et al. 2016), though in general, relatively few mine water management models have been used in mining hydrogeology (Jiang et al. 2013; Lamoreaux et al. 2014; Wu et al. 2010). The hydraulic management model considers the combination of optimizing mine dewatering, water supply, and environmental protection (Jiang et al. 2013; Wu et al. 2006; Yin et al. 2016), while the hydraulic–economic management model maximizes the economic benefit of optimizing mine dewatering, water supply, and environment protection (Wu et al. 2005, 2010, 2017). The management model is mainly used to manage water from the karst aquifer underlying coal seams in northern China (Wu et al. 2005, 2006, 2010). However, these models have not often been used to manage the mine water that originates from a fractured aquifer overlying a coal seam.

We used a hydraulic-economic management model to investigate the Suancigou coal mine in northwestern China. The following steps were used to apply the model: (1) the source of mine water was determined from the hydrogeology; (2) a numerical groundwater model was constructed to determine the critical parameters of the hydraulic-economic management model; and (3) the optimal mine dewatering rate and economic benefit were calculated from the hydraulic-economic management model. This study resolved a problem of mine dewatering, water supply, and environmental protection by improving sustainable development. Simultaneously, the effectiveness of the hydraulic-economic management model was verified by its application in the Suancigou coal mine.

Study Area

The Suancigou underground coal mine is located in Jungar Banner county, Inner Mongolia, northwestern China (Fig. 1). The climate is semi-arid, and rainfall mainly occurs from June to September. The 20-year average precipitation and evaporation are nearly 400 mm/year and ≈ 2100 mm/year, respectively (Cao et al. 2011). The landscape is dominated by hills and the topographic relief is relatively clear.

The Suancigou coal mine is located on a homoclinal structure dipping to the west with an inclination angle of less than 5°; large faults are relatively infrequent in the mine (Figs. 1, 2). The main stratum includes: the Ordovician (O), which is mainly composed of limestone and dolomite; the Carboniferous Benxi group (C_2b), which is dominated by mudstone and shale; the Carboniferous Taiyuan group (C_2t, mudstone with intercalated sandstone); the Permian Shanxi group (P_1s), Xiashihezi group (P_2x), and Shiqianfeng group (P_2sh), which are sandstone with the intercalated mudstone); the Permian Shangshihezi group (P_2s), which is interbedded sandstone-mudstone (Figs. 2, 3), along with the Neogene, and the Quaternary (Fig. 2). The no. 4 coal seam is distributed in P_1s; its thickness ranges from 2.1 to 5.6 m with an average of 4.3 m (Fig. 2). The no. 6 coal seam is distributed in C_2t, and ranges in thickness from 7.0 to 24.9 m, with an average of 13.6 m (Fig. 2).

According to the lithological association, the hydrogeological structure is divided vertically into four aquifers, an aquitard, and an aquiclude (Fig. 3). The spatial relationship of these and the coal seams is shown in Fig. 3. The four aquifers are known as the first, second, third, and fourth aquifer from top to bottom, respectively (Fig. 3). The fourth aquifer is a karst limestone aquifer, while the other three are fractured sandstone with intercalated mudstone. The lithology of the aquitard is interbedded sandstone-mudstone and the lithology of the aquiclude is mudstone and shale.

The hydraulic conductivity and the specific well yield were obtained by a pumping test (Mu et al. 2018). The hydraulic conductivity of the karst aquifer ranged from 0.004 to 76.2 m/day, and the specific well yield ranged from 0.01 to 66.9 L/(s m). Therefore, there is significant heterogeneity

in the permeability and water yield of the karst aquifer. In general, the karst water flows from east to west along the dip direction of the stratum. Meanwhile, the piezometric head of karst water increases from east to west, which also increases the risk of water inrush in this direction. In addition, there is a water source field extracted from the karst aquifer (Fig. 1), which leads to slowly decline of the water table.

The hydraulic conductivity of the third aquifer ranges from 0.0004 to 0.013 m/day, and the specific well yield is about 0.001 L/(s m). The hydraulic conductivity of the second aquifer ranges from 0.002 to 0.03 m/day, and the specific well yield ranges from 0.002 to 0.006 L/(s m). The hydraulic conductivity of the first aquifer ranges from 0.004 to 0.008 m/day, and the specific well yield ranges from 0.003 to 0.03 L/(s m). In general, the hydraulic conductivity of the fracture aquifers is less than 0.05 m/day, and the specific well yield is less than 0.02 L/(s m). On the whole, the permeability of the fracture aquifers is relatively poor, and the water yield property of the fracture aquifers is relatively weak. Therefore, the risk of water inrush from the fractured aquifers is relatively low.

Methodology

The source identification of mine water provide a solid foundation for the groundwater numerical and hydro-economic management models. The groundwater numerical model provides a key parameter, namely the unit impulse response function. The unit impulse response function integrates the groundwater numerical model with the hydro-economic management model of the mine water (Wu et al. 2010; Zhu 2013; Zhu et al. 2014). The hydro-economic management model was used to calculate the configuration scheme of mine dewatering or water supply, along with the maximum economic gains in the management period.

Source Identification of Mine Water

Analysis of Water Sources from the Coal Seam Floor

The analysis of water sources is based on a water inrush coefficient from the coal seam floor. The method of water inrush coefficient is widely used to evaluate water inrush from the coal seam floor in the coal fields of north China (Wu 2014) and considers two main factors: aquiclude thickness and water pressure. The critical value of the water inrush coefficient is regarded as 0.06 MPa/m in the geologic structure area and 0.1 MPa/m in the intact rock mass area (Wu 2014):

$$T = \frac{P}{M} \tag{1}$$

where T is the water inrush coefficient, MPa/m; P is the water pressure sustained by the aquiclude underlying coal seam floors, MPa; and M is the thickness of the aquiclude, m.

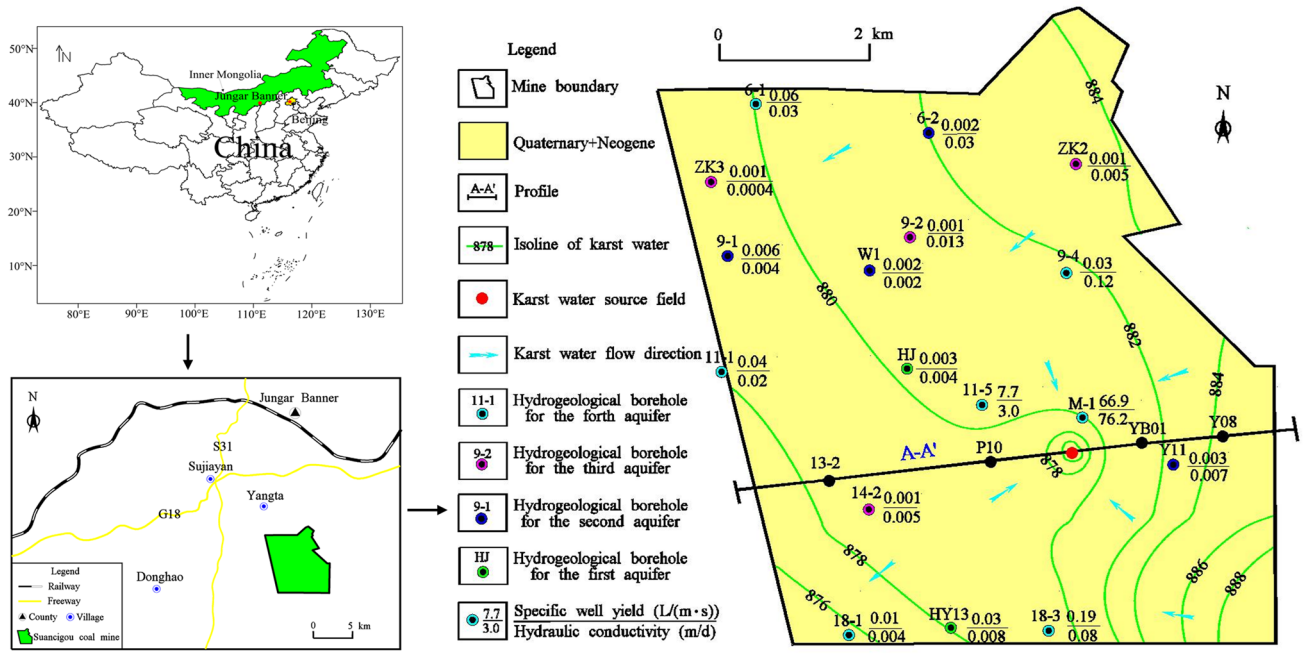

Fig. 1 Location and hydrogeological map of the study area

Analysis of Water Source from a Coal Seam Roof

Deformation and failure of the overlying rock mass is caused by mining collapse, and the overlying rock mass is divided into three zones according to the deformation and failure characteristics (Fig. 4). From bottom to top, these are the caving zone, the fractured zone, and the bending zone, respectively (State Administration of Work Safety et al. 2017). The caving and fractured zones are known as the water-conducting fractured zone in mining hydrogeology. When this zone reaches the aquifer, the groundwater flows into the mine (Fig. 4; State Administration of Work Safety et al. 2017).

Because the uniaxial compression strength of the rock of a coal seam roof ranged from 20 to 40 MPa, the height of the water-conducting fracture zone was calculated by Eq. (2), according to the State Administration of Work Safety et al. (2017):

$$H_{li} = 20\sqrt{\sum M} + 10 \tag{2}$$

where H_{li} is the height of the water-conducting fracture zone, m; and $\sum M$ is the accumulative mining thickness, m.

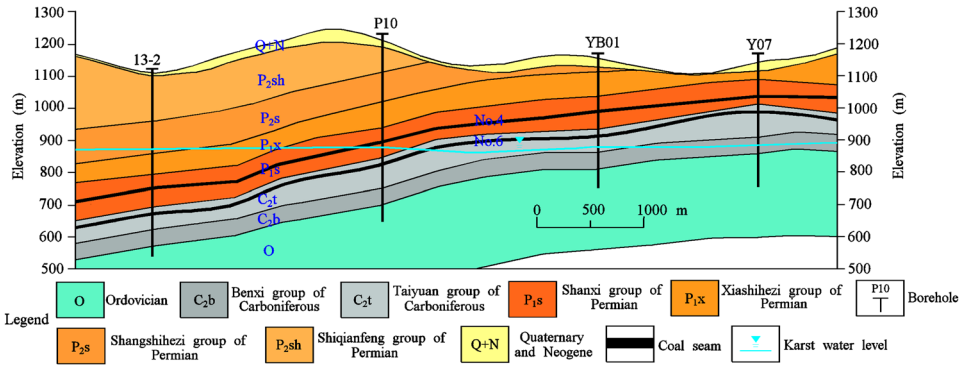

Fig. 2 A-A' hydrogeological profile in Fig. 1

Fig. 3 Hydrogeological columnar section

Hydrogeological structure	Thickness (m)	Columnar	Stratum	Lithology description
The first aquifer	170		Shiqianfeng group of Permian	Sandstone with the intercalated mudstone
Aquitard	200		Shangshihe group of Permian	Interbedded sandstone-mudstone
The second aquifer	100		Xiashihe group of Permian	Sandstone with the intercalated mudstone
No.4 coal seam	4		Shanxi group of Permian	Sandstone with the intercalated mudstone
The third aquifer	40		Taiyuan group of Carboniferous	Mudstone with the intercalated sandstone
No.6 coal seam	14		Benxi group of Carboniferous	Mudstone and shale
Aquiclude	50			
The fourth aquifer	300		Ordovician	Limestone and dolomite

Groundwater Numerical Model

Mathematical Model

The movement of karst and fracture water is reasonably consistent with Darcy's law at the macro-scale (Panagopoulos 2012; Wu et al. 2009). The boundary of the fixed flow is found at the lateral boundaries, and the bottom boundary is regarded as a lower confining bed. The first aquifer is an unconfined aquifer, while the second, third, and fourth aquifers are confined aquifers. The movement of groundwater can be described as a three-dimensional unsteady flow in the anisotropic and heterogeneous media, and its mathematical model is shown in Eq. (3). The positive direction of x, y, and z axes are east, north, and vertical-up in the model, respectively:

$$\begin{cases} \frac{\partial H}{\partial x}\left(K_{xx}M\frac{\partial H}{\partial x}\right)+\frac{\partial H}{\partial y}\left(K_{yy}M\frac{\partial H}{\partial y}\right)+\frac{\partial H}{\partial z}\left(K_{zz}M\frac{\partial H}{\partial z}\right)+w+m=S_sM\frac{\partial H}{\partial t};(x,y,z)\in D,t\geq 0 \\ \frac{\partial H}{\partial x}\left(K_{xx}H\frac{\partial H}{\partial x}\right)+\frac{\partial H}{\partial x}\left(K_{yy}H\frac{\partial H}{\partial y}\right)+\frac{\partial H}{\partial z}\left(K_{zz}H\frac{\partial H}{\partial y}\right)+r=\mu\frac{\partial H}{\partial t};(x,y,z)\in D,t\geq 0 \\ H(x,y,z,t)_{t=0}=H_0(x,y,z);(x,y,z)\in D \\ K_{xx}\frac{\partial H}{\partial x}\cos(n,x)+K_{yy}\frac{\partial H}{\partial y}\cos(n,y)|\Gamma_1=q(x,y,t);(x,y)\in\Gamma_1 \end{cases} \quad (3)$$

where x, y and z are coordinate axes; t is the time (d); D is the model scope; Γ_1 is the boundary of the model scope; K_{xx} is the hydraulic conductivity in x direction (m/day); K_{yy} is the hydraulic conductivity in y direction (m/day); K_{zz} is the hydraulic conductivity in z direction (m/day); M is the aquifer thickness (m); H is the hydraulic head (m); S_s is the specific storage of the confined aquifer (1/m); μ is the specific water yield (nondimensional quantity); q is the unit discharge (m^2/day); n is the unit normal vector of the boundary; w is the amount of water extracted from the karst aquifer (m^3/m^2/day); m is the rate of mine dewatering (m^3/m^2/day); and r is the rainfall recharge (m^3/m^2/day).

Calibration of Numerical Model

The Aqueveo groundwater modeling system (GMS) software was used to construct the groundwater flow model. The GMS solids module was used to create the model's hydrogeological structure and the GMS modular finite-difference module was used with MODFLOW to run the groundwater flow model. The groundwater flow model included six layers and modeled an extent of about 60 km^2. The model is divided into a cube mesh with 167,700 elements and 337,042 nodes; the side length of an element is 100 m (Fig. 5).

The mesh mode was then imported into MODFLOW, which is a core module of GMS, and the MODFLOW code was used to determine the hydraulic conductivity of various hydrogeologic zones and conduct the seepage flow stimulation in the study area (Krcmar and Sracek 2014; Panagopoulos 2012; Zhu et al. 2014). The groundwater flow model was manually calibrated by adjusting the hydraulic conductivity in the zones until the simulated water levels in the four observation wells optimally matched the observed water levels.

Hydro-Economic Management Model

The hydro-economic management model consists of an objective function and constraint conditions (Wu et al. 2005; Zhu et al. 2014). The objective function expresses the maximization of economic benefits, while the constraint conditions express the demand for mine water resources by each user and allowable drawdown of groundwater in the observation wells. The management period in the model was five years, evenly divided into two management periods.

Therefore, the allowable drawdown of groundwater was first identified based on the maximum drawdown of groundwater level from before mining and after. Then, the quantity and quality of demand for mine water by each user was determined. The treatment and transportation costs of mine water, the costs of carrying water, and the price of the water supply were identified by a field survey. Finally, the hydro-economic management model of mine water—that is, the optimized combination of mine dewatering, water supply, and environmental protection—was calculated.

The graded treatment of mine water was carried out according to the water quality requirements of its users (Feng et al. 2014; He et al. 2018; Liu and Liu 2010); it involves underground treatment, primary treatment, and advanced treatment. First, the mine water that is partially purified by the fractured rock mass of the caving zone is used for the preparation plant, this is called as underground treatment (Gu et al. 2016). The remaining mine water is then treated at the land surface; this is known as primary treatment, and includes suppression, filtration, adsorption, and disinfection (He et al. 2018; Liu and Liu 2010; Wu et al. 2017). This water is used for mining equipment, environmental greening and artificial recharge. Finally, the rest of the mine water undergoes intensive treatment. This is known as advanced treatment and involves the use of reverse

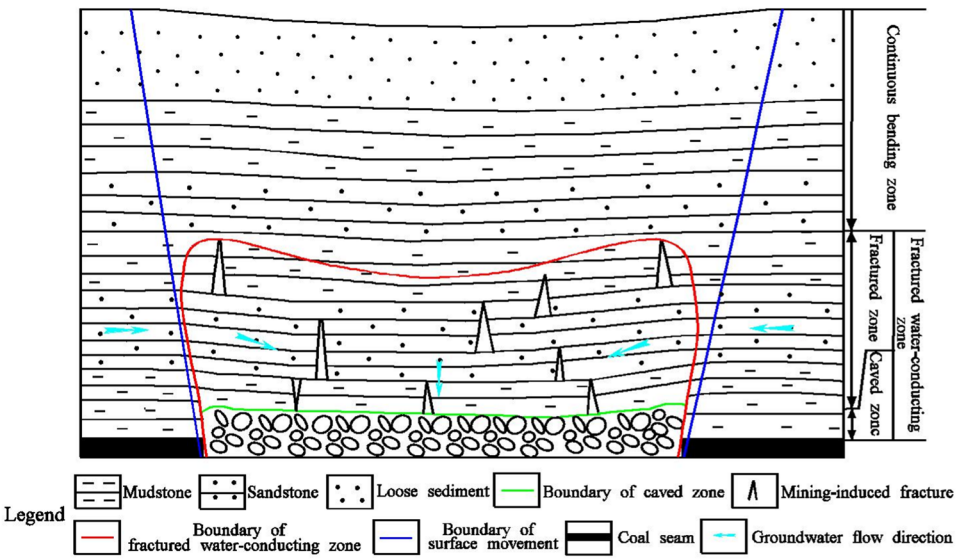

Fig. 4 Sketch map of the fractured water-conducting zone

osmosis film technology (Feng et al. 2014; He et al. 2018; Wu et al. 2017); this water is used for the power plant, the mining equipment, and bathhouse.

Mathematical Model

The mathematical model of mine water management is based on operational research and groundwater management theories and must be established according to the hydrogeology conditions and the use of the mine water. The objective function (Eq. 4) is Wu et al. (2005, 2006, 2010):

$$\begin{aligned} MaxZ = &\sum_{i=1}^{N_1}\sum_{j=1}^{2} C(i,j)\left(gf_1 - tf - cf_1 - cf_2 - sf_1\right)Q_a(i,j) + \sum_{i=1}^{N_2}\sum_{j=1}^{2} C(i,j)\left(gf_2 - tf - cf_1 - cf_2 - sf_2\right)Q_b(i,j) \\ &+ \sum_{i=1}^{N_3}\sum_{j=1}^{2} C(i,j)\left(gf_2 - tf - cf_1 - cf_2 - sf_3\right)Q_c(i,j) + \sum_{i=1}^{N_4}\sum_{j=1}^{2} C(i,j)\left(gf_3 - tf - cf_1 - sf_2\right)Q_d(i,j) \\ &+ \sum_{i=1}^{N_5}\sum_{j=1}^{2} C(i,j)\left(gf_2 - tf - sf_4\right)Q_e(i,j) + \sum_{i=1}^{N_6}\sum_{j=1}^{2} C(i,j)\left(gf_2 - tf - cf_1 - cf_2 - sf_2\right)Q_f(i,j) \\ &+ \sum_{i=1}^{N_7}\sum_{j=1}^{2} C(i,j)\left(gf_2 - tf - cf_1 - sf_5\right)Q_g(i,j) \end{aligned} \tag{4}$$

where Z is the economic benefits; i is the number of the water supply wells, (for example, $i = 1, 2, 3\cdots N_1$); j is the number of the management period, $j = 1, 2$; N_1, N_2, N_3, N_4, N_5, N_6 and N_7 are the quantities of water supply wells for the power plant, mining equipment, bathhouse, dust suppression, artificial recharge, preparation plant and environmental greening, respectively; $Q_a(i,j)$, $Q_b(i,j)$, $Q_c(i,j)$, $Q_d(i,j)$, $Q_e(i,j)$, $Q_f(i,j)$ and $Q_g(i,j)$ are the pumping rate of the water supply well i for the power plant, mining equipment, bathhouse, dust suppression, artificial recharge, preparation plant and environmental greening in the management period j, respectively; gf_1 is the price of water supply for the power plant; gf_2 is the price of water supply for the mining equipment, as well as for the bathhouse and dust suppression; gf_3 is the price of water supply for artificial recharge; tf is the cost of carrying water from the mine to the ground; cf_1 is the cost of the primary treatment; cf_2 is the cost of the advanced treatment; sf_1 is the transportation cost of mine water for the power plant; sf_2 is the transportation cost of mine water for the mining equipment, as well as for dust suppression and artificial recharge; sf_3 is the transportation cost of mine water for the bathhouse; sf_4 is the transportation cost of mine water for the preparation plant; sf_5 is the transportation cost of mine water for environmental greening; and $C(i,j)$ is the length of time water is supplied to each user in the management period.

The constraint conditions of drawdown (Eq. 5) in the mining area in the past and present are as follows Wu et al. (2005, 2006, 2010):

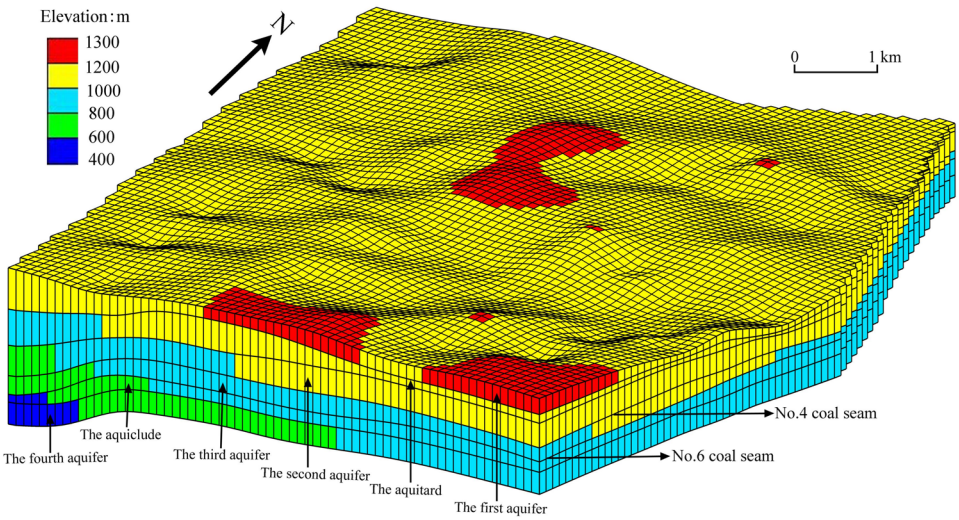

Fig. 5 The mesh for the groundwater numerical model

$$
\begin{cases}
\sum_{i=1}^{N_1}\beta(k,i,1)Q_a(i,1)+\sum_{i=1}^{N_2}\beta(k,i,1)Q_b(i,1)+\sum_{i=1}^{N_3}\beta(k,i,1)Q_c(i,1)+\sum_{i=1}^{N_4}\beta(k,i,1)Q_d(i,1)+\sum_{i=1}^{N_5}\beta(k,i,1)Q_e(i,1) \\
\quad+\sum_{i=1}^{N_6}\beta(k,i,1)Q_f(i,1)+\sum_{i=1}^{N_7}\beta(k,i,1)Q_g(i,1)=s(k,1) \\
\sum_{i=1}^{N_1}\beta(k,i,2)Q_a(i,1)+\sum_{i=1}^{N_1}\beta(k,i,1)Q_a(i,2)+\sum_{i=1}^{N_2}\beta(k,i,2)Q_b(i,1)+\sum_{i=1}^{N_2}\beta(k,i,1)Q_b(i,2)\ +\sum_{i=1}^{N_3}\beta(k,i,2)Q_c(i,1) \\
\quad+\sum_{i=1}^{N_3}\beta(k,i,1)Q_c(i,2)+\sum_{i=1}^{N_4}\beta(k,i,2)Q_d(i,1)+\sum_{i=1}^{N_4}\beta(k,i,1)Q_d(i,2)+\sum_{i=1}^{N_5}\beta(k,i,2)Q_e(i,1)+\sum_{i=1}^{N_5}\beta(k,i,1)Q_e(i,2) \\
\quad+\sum_{i=1}^{N_6}\beta(k,i,2)Q_f(i,1)+\sum_{i=1}^{N_6}\beta(k,i,1)Q_f(i,2)+\sum_{i=1}^{N_7}\beta(k,i,2)Q_g(i,1)+\sum_{i=1}^{N_7}\beta(k,i,1)Q_g(i,2)=s(k,2)
\end{cases}
\tag{5}
$$

where $\beta(k,i,1)$ is the unit impulse response function of the water supply well i on the observation well k (for example, $k=1, 2, 3$ and so on) in the first management period; $\beta(k,i,2)$ is the unit impulse response function of the water supply well i on the observation well k in the second management period; $s(k,1)$ is the allowable drawdown of the observation well k in the first management period; and $s(k,2)$ is the allowable drawdown of the observation well k in the second management period. The physical meanings of the other parameters are the same as in Eq. (4). The constraint conditions of drawdown (Eq. 6) in the mining area in the future are as follows Wu et al. (2005, 2006, 2010):

$$\begin{cases} \sum_{i=1}^{N_1}\beta(k,i,1)Q_a(i,1)+\sum_{i=1}^{N_2}\beta(k,i,1)Q_b(i,1)+\sum_{i=1}^{N_3}\beta(k,i,1)Q_c(i,1)+\sum_{i=1}^{N_4}\beta(k,i,1)Q_d(i,1)+\sum_{i=1}^{N_5}\beta(k,i,1)Q_e(i,1) \\ \quad +\sum_{i=1}^{N_6}\beta(k,i,1)Q_f(i,1)+\sum_{i=1}^{N_7}\beta(k,i,1)Q_g(i,1)\le s(k,1) \\ \sum_{i=1}^{N_1}\beta(k,i,2)Q_a(i,1)+\sum_{i=1}^{N_1}\beta(k,i,1)Q_a(i,2)+\sum_{i=1}^{N_2}\beta(k,i,2)Q_b(i,1)+\sum_{i=1}^{N_2}\beta(k,i,1)Q_b(i,2)+\sum_{i=1}^{N_3}\beta(k,i,2)Q_c(i,1) \\ \quad +\sum_{i=1}^{N_3}\beta(k,i,1)Q_c(i,2)+\sum_{i=1}^{N_4}\beta(k,i,2)Q_d(i,1)+\sum_{i=1}^{N_4}\beta(k,i,1)Q_d(i,2)+\sum_{i=1}^{N_5}\beta(k,i,2)Q_e(i,1)+\sum_{i=1}^{N_5}\beta(k,i,1)Q_e(i,2) \\ \quad +\sum_{i=1}^{N_6}\beta(k,i,2)Q_f(i,1)+\sum_{i=1}^{N_6}\beta(k,i,1)Q_f(i,2)+\sum_{i=1}^{N_7}\beta(k,i,2)Q_g(i,1)+\sum_{i=1}^{N_7}\beta(k,i,1)Q_g(i,2)=s(k,2) \end{cases} \tag{6}$$

where the physical meanings of the parameters are the same as in Eqs. (4) and (5).

The constraint conditions of water supply quantity of each user (Eq. 7) are:

$$\begin{cases} Q_1\le\sum_{i=1}^{N_1}Q_a(i,1)\le Q_2,\ Q_1\le\sum_{i=1}^{N_1}Q_a(i,2)\le Q_2, Q_3\le\sum_{i=1}^{N_2}Q_b(i,1)\le Q_4,\ Q_3\le\sum_{i=1}^{N_2}Q_b(i,2)\le Q_4 \\ Q_5\le\sum_{i=1}^{N_3}Q_c(i,1)\le Q_6,\ Q_5\le\sum_{i=1}^{N_3}Q_c(i,2)\le Q_6, Q_7\le\sum_{i=1}^{N_4}Q_d(i,1)\le Q_8,\ Q_7\le\sum_{i=1}^{N_4}Q_d(i,2)\le Q_8 \\ Q_9\le\sum_{i=1}^{N_5}Q_e(i,1)\le Q_{10},\ Q_9\le\sum_{i=1}^{N_5}Q_e(i,2)\le Q_{10}, Q_{11}\le\sum_{i=1}^{N_6}Q_f(i,1)\le Q_{12},\ Q_{11}\le\sum_{i=1}^{N_6}Q_f(i,2)\le Q_{12} \\ Q_{13}\le\sum_{i=1}^{N_7}Q_g(i,1)\le Q_{14},\ Q_{13}\le\sum_{i=1}^{N_7}Q_g(i,2)\le Q_{14} \end{cases} \tag{7}$$

where Q_1 and Q_2 are the lower and upper limits of the rate of water supply for the power plant, respectively, (m^3/day); Q_3 and Q_4 are the lower and upper limits of the rate of water supply for the mining equipment, respectively, (m^3/day); Q_5 and Q_6 are the lower and upper limits of the rate of water supply for the bathhouse, respectively, (m^3/day); Q_7 and Q_8 are the lower and upper limits of the rate of water supply for dust suppression, respectively, (m^3/day); Q_9 and Q_{10} are the lower and upper limits of the rate of water supply for artificial recharge, respectively, (m^3/day); Q_{11} and Q_{12} are the lower and upper limits of the rate of water supply for the preparation plant, respectively, (m^3/day); and Q_{13} and Q_{14} are the lower and upper limit of the rate of water supply for environmental greening, respectively, (m^3/day).

Unit Impulse Response Function

The water-conducting fractured zone affects the second and third aquifers (Fig. 3), so mine water originates from these two confined aquifers. Moreover, the mathematical model of groundwater movement in these two aquifers is described in Eq. (8) (Mu et al. 2018):

$$\begin{cases} \frac{\partial h}{\partial x}\left(K_{xx}M\frac{\partial h}{\partial x}\right)+\frac{\partial h}{\partial y}\left(K_{yy}M\frac{\partial h}{\partial y}\right)+\frac{\partial h}{\partial z}\left(K_{zz}M\frac{\partial h}{\partial z}\right)+l+p=S_sM\frac{\partial h}{\partial t};(x,y,z)\in D,t\ge 0 \\ h(x,y,z,t)_{t=0}=h_0(x,y,z);(x,y,z)\in D \\ K_{xx}\frac{\partial h}{\partial x}\cos(n,x)+K_{yy}\frac{\partial h}{\partial y}\cos(n,y)|\Gamma_1=q(x,y,t);(x,y)\in\Gamma_1 \end{cases} \tag{8}$$

where l is leakage recharge; and p is the specific rate of flow for pumping water. The physical meaning of the other parameters is the same as in Eq. (3). Supposing $h = H + s$, Eq. (8) is converted into Eq. (9) and Eq. (10) according to the superposition principle. Equations (9) and (10) are:

$$\begin{cases} \frac{\partial H}{\partial x}(K_{xx}M\frac{\partial H}{\partial x}) + \frac{\partial H}{\partial y}(K_{yy}M\frac{\partial H}{\partial y}) + \frac{\partial H}{\partial z}(K_{zz}M\frac{\partial H}{\partial z}) + l = S_sM\frac{\partial H}{\partial t}; (x,y,z) \in D, t \geq 0 \\ H(x,y,z,t)_{t=0} = H_0(x,y,z); (x,y,z) \in D \\ K_{xx}\frac{\partial H}{\partial x}\cos(n,x) + K_{yy}\frac{\partial H}{\partial y}\cos(n,y)|\Gamma_1 = q(x,y,t); (x,y) \in \Gamma_1 \end{cases} \quad (9)$$

where H is the hydraulic head (m) and:

$$\begin{cases} \frac{\partial s}{\partial x}\left(K_{xx}M\frac{\partial s}{\partial x}\right) + \frac{\partial s}{\partial y}\left(K_{yy}M\frac{\partial s}{\partial y}\right) + \frac{\partial s}{\partial z}\left(K_{zz}M\frac{\partial s}{\partial z}\right) + p = S_sM\frac{\partial s}{\partial t}; (x,y,z) \in D, t \geq 0 \\ s(x,y,z,t)_{t=0} = 0; (x,y,z) \in D \\ K_{xx}\frac{\partial s}{\partial x}\cos(n,x) + K_{yy}\frac{\partial s}{\partial y}\cos(n,y)|\Gamma_1 = 0; (x,y) \in \Gamma_1 \end{cases} \quad (10)$$

where s is the drawdown (m).

The governing differential equation, the initial conditions, and the boundary conditions are homogenous in Eq. (10). Therefore, Eq. (10) is used to calculate the unit impulse response function, which is the critical parameter of the management model of mine water.

According to Eq. (10), the calibrated groundwater numerical model in the "Source Identification of Mine Water" section is modified by the boundary and initial conditions, and by the source/sink term. The modified numerical model is then used to calculate the unit impulse response function. The drawdown of the observation well is obtained when the wells pump water with a specific rate of flow in the first management period, and the drawdown is the unit impulse response function in the first management period (Wu et al. 2010; Zhu et al. 2014). On this basis, the residual drawdown of the observation wells is obtained when the wells stop pumping water in the second management period, and the residual drawdown is the unit impulse response function in the second management period. The specific rate of flow was set as 150 m^3/day in this study, according to the hydrogeological conditions. The unit impulse response function under the specific rate of flow is shown in Table 1 and supplemental Table S-1.

Hydraulic and Economic Parameters

The demand for mine water resources by each user, according to the field survey, is shown in Table 2. The users include the power plant, mining equipment, bathhouse, dust suppression, artificial recharge, preparation plant, and environmental greening. The allowable drawdown of the observation wells in the entire management period is shown in Table 3.

Table 4 shows the costs of water supply for each user, according to the field survey, the costs of carrying water from the mine to the surface, and primary and advanced treatment; and the transportation costs for power plant, mining equipment, bathhouse, dust suppression, artificial recharge, preparation plant, and environmental greening.

The data in Tables 2, 3 and 4 were applied to the mine water management model and the simplex method was used to solve this model (Wu et al. 2005, 2006).

Results and Discussion

Source of Mine Water

As shown in Fig. 3, the karst aquifer underlies the no. 4 and no. 6 coal seams. The water inrush coefficient of the no. 4 coal seam ranges from 0 to 0.024 MPa/m (Fig. 6a), and the water inrush coefficient gradually increases from east to west with the increase of piezometric level (Figs. 2, 6a). The water inrush coefficient of the no. 6 coal seam ranges from 0 to 0.04 MPa/m (Fig. 6b), and the water inrush coefficient gradually increases from east to west with the increase of piezometric level (Figs. 2, 6b). Obviously, the water inrush coefficient is less than the critical water inrush coefficient of 0.06 MPa/m, for either the no. 4 or no. 6 coal seams. Although the karst aquifer is a confined aquifer, there is little chance of water inrush from the coal seam floor because of the relatively low water inrush coefficient. In addition, at the Suancigou coal mine, the karst water aquifer below the no. 6 coal seam is not a major source of mine water.

The water-conducting fracture zone is an important channel for groundwater entering the mine from the coal seam roof. The computed result indicates that the height of the water-conducting fracture zone ranged from 38.6 to 59.8 m with an average of 51.7 m after the no. 4 coal seam was mined, and this affected the second aquifer (Fig. 3). The height of the water-conducting fracture zone ranged from 63.1 to 109.8 m with an average of 83.1 m after the no. 6 coal seam had been mined, and this affected the second

Table 1 Unit impulse response function in the hydro-economic management model (unit: m)

k	1		2		3		4		5		6	
i / j	1	2	1	2	1	2	1	2	1	2	1	2
1	96.7	0.48	2.7	0.29	0.32	0.11	0.08	0.05	4.7	0.39	1.3	0.22
2	2.7	0.29	87.9	0.8	2.3	0.36	0.17	0.07	1.4	0.24	2.74	0.38
3	0.31	0.11	1.8	0.38	108.5	1.32	1.1	0.27	0.24	0.11	0.8	0.21
4	0.08	0.06	0.18	0.08	1.4	0.3	112.4	1.0	0.09	0.07	0.12	0.06
5	4.50	0.39	1.34	0.24	0.24	0.12	0.09	0.06	100	0.68	3.12	0.37
6	1.30	0.22	3.15	0.36	0.86	0.21	0.14	0.07	3.2	0.36	97	0.67
7	0.26	0.11	1.19	0.31	3.39	0.66	0.69	0.23	0.4	0.16	2.19	0.41
8	0.08	0.06	0.13	0.08	0.52	0.17	1.72	0.35	0.11	0.08	0.22	0.1
9	0.89	0.19	0.44	0.15	0.18	0.11	0.1	0.08	4.5	0.33	1.7	0.27
10	0.47	0.16	0.49	0.17	0.29	0.13	0.13	0.08	1.8	0.3	2.96	0.42
11	0.2	0.12	0.3	0.13	0.39	0.15	0.22	0.1	0.5	0.19	1.16	0.27
12	0.11	0.1	0.13	0.1	0.24	0.16	0.3	0.14	0.17	0.13	0.28	0.15
13	0.40	0.2	0.24	0.1	0.14	0.1	0.1	0.08	1.52	0.23	0.8	0.18
14	0.32	0.15	0.27	0.14	0.23	0.12	0.13	0.09	1.08	0.22	1.04	0.23
15	0.22	0.15	0.22	0.14	0.22	0.13	0.17	0.11	0.49	0.2	0.59	0.21
16	0.17	0.13	0.16	0.12	0.19	0.12	0.17	0.11	0.27	0.17	0.31	0.16
17	0.18	0.11	0.13	0.09	0.1	0.08	0.08	0.07	0.48	0.15	0.29	0.12
18	0.19	0.12	0.15	0.11	0.12	0.09	0.1	0.08	0.47	0.17	0.36	0.15
19	0.21	0.15	0.19	0.14	0.17	0.12	0.15	0.11	0.4	0.2	0.38	0.18
20	0.17	0.15	0.15	0.13	0.13	0.1	0.13	0.1	0.25	0.18	0.24	0.16
21	0.08	0.08	0.07	0.07	0.06	0.06	0.05	0.06	0.12	0.1	0.09	0.1
22	0.07	0.07	0.06	0.06	0.05	0.05	0.05	0.05	0.09	0.09	0.07	0.07
23	0.11	0.1	0.09	0.09	0.08	0.08	0.07	0.07	0.13	0.13	0.1	0.1
24	0.09	0.1	0.08	0.08	0.06	0.07	0.06	0.06	0.11	0.11	0.09	0.11
25	0.14	0.14	0.12	0.12	0.1	0.11	0.09	0.09	0.17	0.17	0.14	0.14
26	0.17	0.17	0.14	0.14	0.12	0.13	0.11	0.11	0.21	0.21	0.16	0.17
27	6.23	0.37	0.72	0.15	0.14	0.07	0.06	0.04	3.0	0.32	0.54	0.14
28	14.4	0.54	4.6	0.43	0.42	0.13	0.07	0.04	3.75	0.39	1.76	0.27
29	0.59	0.17	5.22	0.8	9.31	1.3	0.42	0.14	0.36	0.16	1.23	0.32
30	0.1	0.06	0.46	0.15	6.06	0.82	5.9	0.72	0.09	0.06	0.26	0.1
31	2.45	0.27	0.53	0.15	0.14	0.08	0.07	0.06	8.16	0.44	1.08	0.21
32	3.6	0.42	1.8	0.31	0.31	0.12	0.08	0.05	16.7	0.92	5.14	0.54
33	0.41	0.13	1.62	0.34	1.63	0.37	0.25	0.1	0.82	0.2	5.9	0.66
34	0.11	0.08	0.33	0.15	1.6	0.39	1.56	0.38	0.17	0.11	0.57	0.2
35	0.71	0.18	0.28	0.12	0.12	0.09	0.08	0.07	3.0	0.36	0.78	0.2
36	0.82	0.19	0.51	0.16	0.2	0.11	0.11	0.08	4.44	0.35	2.25	0.32
37	0.28	0.12	0.37	0.14	0.33	0.14	0.15	0.08	0.92	0.23	2.0	0.36
38	0.13	0.11	0.18	0.1	0.34	0.17	0.29	0.13	0.24	0.15	0.4	0.21
39	0.36	0.14	0.2	0.11	0.12	0.09	0.09	0.08	1.31	0.21	0.51	0.16
40	0.4	0.15	0.26	0.13	0.16	0.1	0.11	0.08	1.6	0.23	0.9	0.2
41	0.27	0.14	0.24	0.13	0.2	0.12	0.14	0.09	0.78	0.21	0.84	0.22
42	0.17	0.14	0.17	0.13	0.18	0.13	0.16	0.11	0.3	0.19	0.37	0.19
43	0.21	0.11	0.14	0.09	0.1	0.08	0.08	0.07	0.65	0.16	0.32	0.12
44	0.19	0.11	0.14	0.1	0.1	0.08	0.08	0.07	0.55	0.16	0.34	0.13
45	0.2	0.13	0.17	0.11	0.14	0.1	0.12	0.09	0.48	0.18	0.44	0.16
46	0.18	0.14	0.16	0.13	0.15	0.11	0.13	0.1	0.3	0.18	0.29	0.16

Note: This table provides the partial results because of length limitation. All results is shown in supplemental materials Table S-1, i is the number of the water supply wells, (for example, i = 1, 2, 3 and so on); j is the number of the management period, j = 1, 2; k is the number of the observation well, (for example, i = 1, 2, 3 and so on)

Table 2 User demand for mine water resources in the hydro-economic management model (unit: m^3/day)

User	Ranges	Users	Ranges	User	Ranges
Power plant	1500–2500	Mining equipment	800–1200	Bathhouse	100–300
Dust precipitation	800–1200	Artificial recharge	0–2000	Preparation plant	700–1000
Environmental greening	50–300				

and third aquifers (Fig. 3). Evidently, mine water originating from the second aquifer overlaid the no. 4 coal seam and third aquifer overlaid the no.6 coal seam. Because the yield property of the sandstone fracture aquifers is relatively weak, the rate of mine dewatering is relatively low.

Validation of the Groundwater Numerical Model

The hydrogeological parameters of the groundwater numerical model are identified when the calculated water level is well matched with a measured water level in the observation wells (Figs. 7, 8, Table 5). Figure 8 shows the measured and calculated water levels in the observation wells. As shown in Fig. 8, there is a good match between the calculated and measured water levels at early times, which may be due to the selection of initial head conditions. Due to the observation wells being close to the fixed-flow lateral boundaries of the model (except for well 11-5), the goodness of fit between calculated and measured water levels at later times is relatively weak compared with that at early times. Considering the complexity of the hydrogeologic conditions, we think that the modeled water levels are generally consistent with the measured water levels, which shows that the established numerical model of groundwater has a relatively satisfactory accuracy for use in this case study of water use optimization.

The unit impulse response function is the critical parameter of the hydro-economic management model; therefore, the reliability of the hydro-economic management model partly depends on the computed result of the unit impulse response function. Meanwhile, the unit impulse response function is determined according to the groundwater numerical model. Briefly speaking, the reliability of the hydro-economic management model is closely related to the validity of the groundwater numerical model. According to our validation results, the hydro-economic management model should be credible. For the record, the boundary conditions and calculation parameters of the groundwater numerical model inevitably exist a certain degree of uncertainty because of the complex hydrogeological condition. The impact of this uncertainty on the unit impulse response function was not considered in this paper but will be investigated in future studies.

Optimizing Mine Water Management

The configuration scheme of mine water resources was obtained using the optimization results of the hydro-economic management model (Table 6). The rate of the water supply for the power plant, mining equipment, bathhouse, dust suppression, artificial recharge, preparation plant, and environmental greening was respectively 2046, 250, 156, 286, 1110, 1082, and 1160 (m^3/day) in the first management period and 2178, 245, 198, 262, 1142, 834, 817 (m^3/day) in the second management period. The total rate of mine dewatering or water supply was 6097 m^3/day in the first management period and 5677 m^3/day in the second management period. The average rate of mine dewatering or water supply was 5887 m^3/day in the entire management period. Dewatering in advance of mining enhances mine safety against water inrushes from aquifers above the coal extraction area. Obviously, the average rate of mine dewatering is relatively low, which is consistent with the source analysis results, which further proves the validity of the hydro-economic management model.

Table 3 Allowable drawdown of the observation wells in the hydro-economic management model (unit: m)

Observation wells	Allowable drawdown	Observation wells	Allowable drawdown	Observation wells	Allowable drawdown
1	176	18	180	35	136
2	145	19	154	36	104
3	99	20	128	37	86
4	95	21	172	38	60
5	170	22	153	39	144
6	152	23	132	40	128
7	107	24	136	41	97
8	92	25	104	42	72
9	177	26	91	43	145
10	144	27	123	44	127
11	134	28	97	45	106
12	102	29	49	46	93
13	181	30	46	47	78
14	167	31	127	48	128
15	101	32	99	49	95
16	143	33	66	50	109
17	185	34	45		

Table 4 Economic parameters in the hydro-economic management model (unit: CNY/m^3)

Items	Powerplant	Mining equipment	Bathhouse	Artificial recharge	Preparation plant	Dust suppression	Environmentalgreening
Water supply price	6.0	5.6	5.6	0.0	5.6	5.6	5.6
Carrying water cost	0.87	0.87	0.87	0.87	0.87	0.87	0.87
Primary treatment cost	0.68	0.68	0.68	0.68	0.0	0.68	0.68
Advanced treatment cost	0.93	0.93	0.93	0.0	0.0	0.0	0.0
Transportation cost	0.16	0.0	0.8	0.0	0.2	0.0	1.2

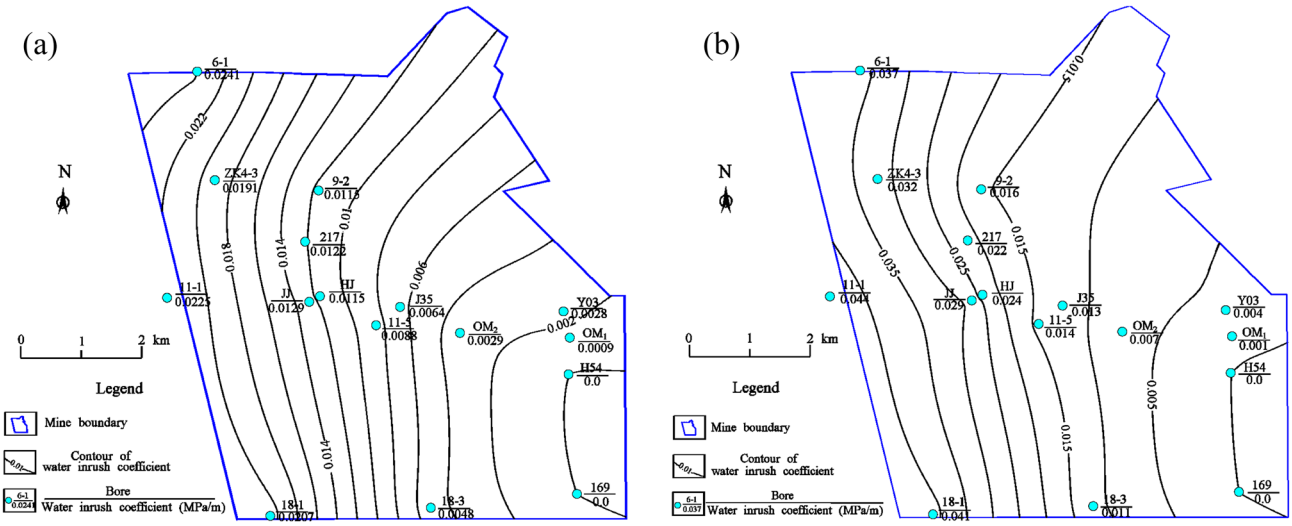

Fig. 6 Contour of water inrush coefficient of coal seams: **a** No. 4 coal seam; **b** No.6 coal seam

In addition, the maximum direct economic gains was obtained according to the optimization results of the hydro-economic management model. The cumulative maximum direct economic gain was CNY 36.6 million in the entire management period. The annual average direct economic gain was CNY 7.3 million. In addition, mine water treatment extends the life of mining equipment and because of this, the annual average indirect economic gain was CNY 2.3 million. Finally, the annual average economic gain was CNY 9.6 million. The optimization results show that applying the hydro-economic management model can produce a lucrative economic income, while also meeting the demand of water resources for users, which is conducive to breaking down barriers between mines and other enterprises, e.g. power plants. More importantly, this measure reduces the environmental pollution caused by random discharge of mine water (Guo et al. 2019).

The hydro-economic management model of mine water integrates the groundwater numerical and optimization models. It provides a relatively satisfactory solution to allow efficient utilization of mine water resources, environmental and groundwater resource protection, and zero release of mine water by the effective combination of mine dewatering, water supply and environmental greening (He et al. 2008; Lamoreaux et al. 2014; Wu 2014; Wu et al. 2010, 2017),

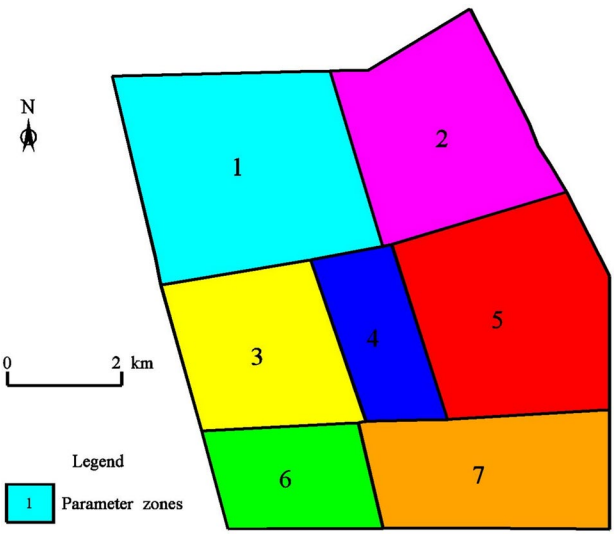

Fig. 7 Hydrogeological parameter zones in the fourth aquifer

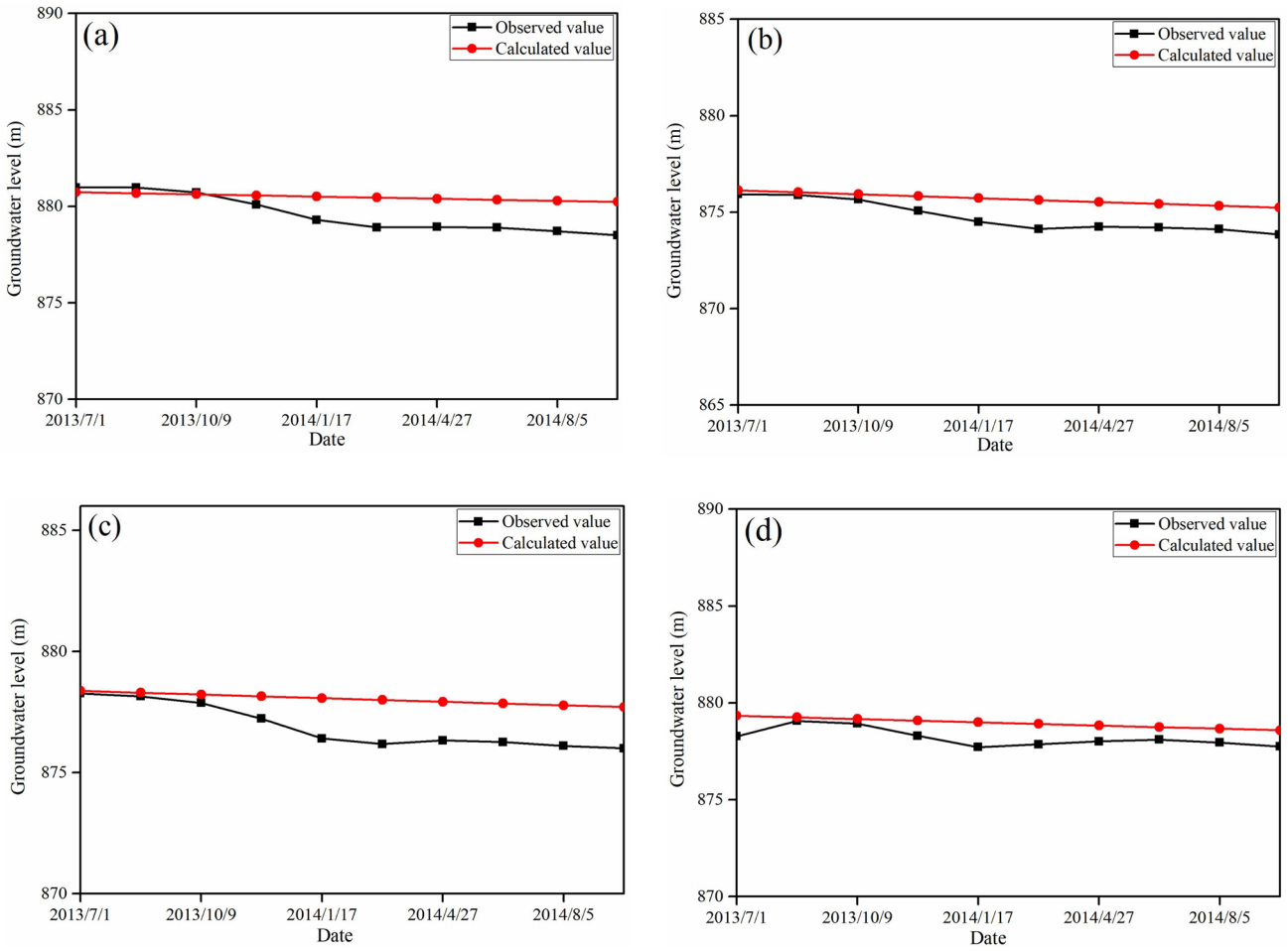

Fig. 8 Comparison of measured water level and calculated water level in the observation wells: **a** 6-1; **b** 18-1; **c** 11-1; and **d** 11-5

Table 5 Hydrogeological parameters of the fourth aquifer in the numerical model

Parameter zones	Hydraulic conductivity in x direction K_{xx} /(m/day)	Hydraulic conductivity in y direction K_{yy} /(m/day)	Hydraulic conductivity in z direction K_{zz} /(m/day)	Specific storage S_s /(1/m)
1	1.5	1.5	0.15	1.5×10^{-5}
2	5.0	5.0	0.5	5.0×10^{-5}
3	2.0	2.0	0.2	2.0×10^{-5}
4	2.2	2.2	0.22	1.5×10^{-5}
5	3.0	3.0	0.3	3.0×10^{-5}
6	1.8	1.8	0.18	1.8×10^{-5}
7	2.5	2.5	0.25	2.5×10^{-5}

which promotes application of the management model. In contrast to other models (Wu et al. 2005, 2006, 2010; Yin et al. 2016), this study proposes a hydro-economic management model for management of mine water from the coal seam roof, and its effectiveness has been verified by its application in the Suancigou coal mine in northwestern China. Similar hydrogeological conditions can be found in other northwestern China mines, which provides a solid foundation for its broad application prospects.

There are abundant coal resources in northwestern China, accounting for at least 60% of the country's total reserves (He et al. 2008; Sun et al. 2012). However, water resources are scarce, the environment is fragile, and the regional economy is underdeveloped (Gu et al. 2016; Wu 2014; Wu et al.

Table 6 Rate of water supply to each user in the hydro-economic management period (unit: m^3/day)

Users	The first period	The second period	Users	The first period	The second period
Power plant	2046	2178	Mining equipment	1110	1142
Bathhouse	250	245	Dust suppression	1082	834
Artificial recharge	156	198	Preparation plant	1160	817
Environmental greening	286	262			

2017). Unfortunately, the exploitation of coal resources is accompanied by the wasting of water resources, environmental pollution, and water supply shortages (Gao et al. 2014; Sun et al. 2012). Meanwhile, local social and economic development depends on the exploitation of coal resources. In addition, national laws and regulations clearly encourage the improvement of mine water utilization rates, especially in areas experiencing water shortages. Mine water must, therefore, be managed to enable the sustainable development of this coal-rich area of northwestern China (Feng et al. 2014; Gao et al. 2014; Hancock and Wolkersdorfer 2012; He et al. 2008; Liu and Liu 2010; Sun et al. 2012; Wu 2014; Wu et al. 2017).

Conclusions

The sources of mine water was identified according to the water inrush coefficient and the height of the water-conducting fracture zone. Meanwhile, the established numerical model of groundwater was calibrated according to water level observation. These achievements provided a solid foundation for establishing the hydro-economic management model.

Based on the theories of groundwater numerical simulation and operational research, we established the hydro-economic model for optimizing management of mine water. Its effective was certified in the Suancigou coal mine of northwest China. Applying the hydro-economic management model can reduce the risk of water inrush, while also achieving efficient use of mine water, relieving the pressure on water supply, and protecting the environment.

In addition, application of the management model also can produce considerable economic returns and social benefit, which will promote popularization of the technology. Therefore, it may reasonably be concluded that this management model has a significant practical importance for the sustainable and efficient development of coal resources, especially in northwestern China.

Supplementary Information The online version contains supplementary material available at https://doi.org/10.1007/s10230-022-00894-3.

Acknowledgements This research was financially supported by the Fundamental Research Funds for the Central Universities (Grant 2-9-2020-019), the Inner Mongolia Science and Technology Major Project (Grant 2020ZD0020), the National Natural Science Foundation of China (Grant 41972259), and the Open Project Program of the Shandong Provincial Lunan Geo-engineering Exploration Institute (Grant LNY2020-Z01). The authors also thank the editor and reviewers for their helpful suggestions.

References

Ardejani FD, Singh RN, Baafi E, Porter I (2003) A finite element model to: 1 predict groundwater inflow to surface mining excavations. Mine Water Environ 22(1):31–38

Cao XM, Liu ZH, Yang ZM, Xu L, Zhang XP (2011) Rainfall characteristics research of spatial and temporal variation in the middle of the loess plateau. J Sichuan Normal Univ (nat Sci) 34(5):724–728

Feng QY, Li T, Qian B, Zhou L, Gao B, Yuan T (2014) Chemical characteristics and utilization of coal mine drainage in China. Mine Water Environ 33(3):276–286

Gao L, Barrett D, Chen Y, Zhou MW, Cuddy S, Paydar Z, Renzullo L (2014) A systems model combining process-based simulation and multi-objective optimisation for strategic management of mine water. Environ Model Softw 60:250–264

Gong HL, Li ML, Hu XL (2000) Management of groundwater in Zhengzhou City, China. Water Resour 34(1):57–62

Gu DZ, Zhang Y, Gao ZG (2016) Technical progress of water resource protection and utilization by coal mining in China. Coal Sci Techno 44(1):1–7 (**in Chinese**)

Guo JS, Ma LQ, Zhang DS (2019) Management and utilization of high-pressure floor-confined water in deep coal mines. Mine Water Environ 38(4):780–797

Hancock S, Wolkersdorfer C (2012) Renewed demands for mine water management. Mine Water Environ 31(2):147–158

He XW, Yang J, Shao LN, Li FQ, Wang X (2008) Problem and countermeasure of mine water resource regeneration in China. J China Coal Soc 33(1):63–66 (**in Chinese**)

He XW, Zhang XH, Li FQ, Zhang CH (2018) Comprehensive utilization system and technical innovation of coal mine water resources. Coal Sci Technol 46(9):9–16 (**in Chinese**)

Jiang SM, Kong XL, Ye H, Zhou NQ (2013) Groundwater dewatering optimization in the Shengli no 1 open-pit coalmine, Inner Mongolia, China. Environ Earth Sci 69(1):187–196

Krcmar D, Sracek O (2014) MODFLOW-USG: the new possibilities in mine hydrogeology modelling (or what is not written in the manuals). Mine Water Environ 33(4):376–383

Lamoreaux JW, Wu Q, Zhou WF (2014) New development in theory and practice in mine water control in China. Carbonate Evaporite 29(2):141–145

Liu HB, Liu ZL (2010) Recycling utilization patterns of coal mining waste in China. Resour Conserv Recy 54(12):1331–1340

Ma ZM, Wu Q, Fu SH (2004) Sustainable utilization management model for groundwater resources. J Hydraul Eng 9:65–69 (**in Chinese**)

Mu WP, Wu Q, Xing Y, Qian C, Wang Y, Du YZ (2018) Using numerical simulation for the prediction of mine dewatering from a karst water system underlying the coal seam in the Yuxian Basin, northern China. Environ Earth Sci 77(5):1–19

Panagopoulos G (2012) Application of MODFLOW for simulating groundwater flow in the Trifilia karst aquifer. Greece Environ Earth Sci 67(7):1877–1889

Rapantova N, Grmela A, Vojtek D, Halir J, Michalek B (2007) Ground water flow modelling applications in mining hydrogeology. Mine Water Environ 26(4):264–270

Singh A, Bürger CM, Cirpka OA (2013) Optimized sustainable groundwater extraction management: general approach and application to the city of Lucknow. India Water Resour Manag 27(12):4349–4368

State Administration of Work Safety, National Energy Administration, National Railway Administration (2017) Rules for the coal pillars establishment and coal mining under buildings, water bodies, railways and main roadways. China Coal Industry Publishing House, Beijing (**in Chinese**)

Sun WJ, Wu Q, Dong DL, Jiao J (2012) Avoiding coal-water conflicts during the development of China's large coal-producing regions. Mine Water Environ 31(1):74–78

Theodossiou NP (2004) Application of non-linear simulation and optimisation models in groundwater aquifer management. Water Resour Manag 18(2):125–141

Wu Q (2014) Progress, problems and prospects of prevention and control technology of mine water and reutilization in China. J China Coal Soc 39(5):795–805 (**in Chinese**)

Wu Q, Zhou WF (2008) Prediction of inflow from overlying aquifers into coalmines: a case study in Jinggezhuang coal mine, Kailuan, China. Environ Geol 55(4):775–780

Wu Q, Dong DL, Shi ZH, Wu X, Sun WD, Ye GJ, Li SW, Liu JT (2000) Optimum combination of water drainage, water supply and eco-environment protection in coal-accumulated basin of North China. Sci China Ser D 43(2):122–133

Wu Q, Dong DL, Di ZQ, Miao Y, Zhao SQ, Guo QW (2005) Combination of drainage, water supply and environmental protection as well as rational distribution of water resource in Zhengzhou mining district. Sci China Ser D 48(10):1768–1779

Wu Q, Zhou WF, Li D, Di ZQ, Miao Y (2006) Management of karst water resources in mining area: dewatering in mines and demand for water supply in the Dongshan Mine of Taiyuan, Shanxi Province, North China. Environ Geol 50(8):1107–1117

Wu Q, Zhou WF, Pan GY, Ye SY (2009) Application of a discrete-continuum model to karst aquifers in North China. Ground Water 47(3):453–461

Wu Q, Hu BX, Wan L, Zheng CM (2010) Coal mine water management: optimization models and field application in North China. Hydrol Sci J 55(4):609–623

Wu Q, Liu YZ, Zhou WF, Li BY, Zhao B, Liu SQ, Sun WJ, Zeng YF (2015) Evaluation of water inrush vulnerability from aquifers overlying coal seams in the Menkeqing coal mine, China. Mine Water Environ 34(3):258–269

Wu Q, Shen JJ, Wang Y (2017) Mining techniques and engineering application for "coal-water" dual-resources mine. J China Coal Soc 42(1):8–16 (**in Chinese**)

Yin SX, Han Y, Chang HY (2016) Study on optimal allocation of karst water resources in Hanxing mining area. Coal Sci Technol 44(8):20–34 (**in Chinese**)

Zeng YF, Wu Q, Liu SQ, Zhai YL, Zhang W (2018) Evaluation of a coal seam roof water inrush: case study in the Wangjialing coal mine, China. Mine Water Environ 37(1):174–184

Zhu B (2013) Management strategy of groundwater resources and recovery of over-extraction drawdown funnel in Huaibei City, China. Water Resour Manag 27(9):3365–3385

Zhu B, Yang JW, Wu Q (2014) Aquifer system incremental linear property and its application on groundwater management. Environ Earth Sci 71(5):2373–2389